Quantizers with Parameterized Distortion Measures

Jun Guo, Philipp Walk, and Hamid Jafarkhani

Center for Pervasive Communications and Computing

University of California, Irvine, CA 92697-2625

{guoj4,pwalk,hamidj}@uci.edu

Abstract

In many quantization problems, the distortion function is given by the Euclidean metric to measure the distance of a source sample to any given reproduction point of the quantizer. We will in this work regard distortion functions, which are additively and multiplicatively weighted for each reproduction point resulting in a heterogeneous quantization problem, as used for example in deployment problems of sensor networks. Whereas, normally in such problems, the average distortion is minimized for given weights (parameters), we will optimize the quantization problem over all weights, i.e., we tune or control the distortion functions in our favor. For a uniform source distribution in one-dimension, we derive the unique minimizer, given as the uniform scalar quantizer with an optimal common weight. By numerical simulations, we demonstrate that this result extends to two-dimensions where asymptotically the parameter optimized quantizer is the hexagonal lattice with common weights. As an application, we will determine the optimal deployment of unmanned aerial vehicles (UAVs) to provide a wireless communication to ground terminals under a minimal communication power cost. Here, the optimal weights relate to the optimal flight heights of the UAVs.

I. Introduction

For a set $\Omega \subset \mathbb{R}^d$ in $d = 1, 2$ dimensions, a quantizer is given by N reproduction or quantization points $\mathbf{Q} = \{\mathbf{q}_1, \ldots, \mathbf{q}_N\} \subset \Omega$ associated with N quantization regions $\mathcal{R} = \{\mathcal{R}_1, \ldots, \mathcal{R}_N\} \subset \Omega$, defining a partition of Ω. To measure the quality of a given quantizer, the Euclidean distance between the source samples and reproduction points is commonly used as the distortion function. We will study quantizers with parameter depending distortion functions

which minimize the average distortion over Ω for a given continuous source sample distribution $\lambda : \Omega \to [0, 1]$, as investigated for example in [1]–[3] with a fixed set of parameters. Contrary to a fixed parameter selection, we will assign to each quantization point variable parameters to control the distortion function of the each quantization point individually. Such controllable distortion functions widens the scope of quantization theory and allows one to apply quantization techniques to many parameter dependent network and locational problems. In this work, we will consider for the distortion function of $\mathbf{q}_n$ a Euclidean square-distance, which is multiplicatively weighted by some $a_n > 0$ and additively weighted by some $b_n > 0$. Furthermore, we exponentially weight all distortion functions by some fixed exponent $\gamma \geq 1$. To minimize the average distortion, the optimal quantization regions are known to be generalized Voronoi (Möbius) regions, which can be non-convex and disconnected sets [4]. In many applications, as in sensor or vehicle deployments, the optimal weights and parameters are usually unknown, but adjustable, and one wishes therefore to optimize the deployment over all admissible parameter values, see for example [3]. We will characterize such *parameter optimized quantizers* over one-dimensional convex target regions, i.e., over closed intervals. As a motivation, we will demonstrate such a parameter driven quantizer for an unmanned aerial vehicle (UAV) deployment to provide energy-efficient communication to ground terminals in a given target region Ω. Here, the parameters relate to the UAVs flight heights.

a) Notation: By $[N] = \{1, 2, \ldots, N\}$ we denote the first N natural numbers, $\mathbb{N}$. We will write real numbers in $\mathbb{R}$ by small letters and row vectors by bold letters. The Euclidean norm of $\mathbf{x}$ is given by $\|\mathbf{x}\| = \sqrt{\sum_n x_n^2}$. The open ball in $\mathbb{R}^d$ centered at $\mathbf{c} \in \mathbb{R}^d$ with radius $r \geq 0$ is denoted by $\mathcal{B}(\mathbf{c}, r) = \{\boldsymbol{\omega} \mid \|\boldsymbol{\omega} - \mathbf{c}\|^2 \leq r\}$. We denote by $\mathcal{V}^c$ the complement of the set $\mathcal{V} \subset \mathbb{R}^d$. The positive real numbers are denoted by $\mathbb{R}_+ := \{a \in \mathbb{R} \mid a > 0\}$. Moreover, for two points $\mathbf{a}, \mathbf{b} \in \mathbb{R}^d$, we denote the generated half space between them, which contains $\mathbf{a} \in \mathbb{R}^d$, as $\mathcal{H}(\mathbf{a}, \mathbf{b})$.

II. SYSTEM MODEL

To motivate the concept of parameterized distortion measures, we will investigate the deployment of N UAVs positioned at $\mathbf{P} = \{\mathbf{p}_1, \ldots, \mathbf{p}_N\} \subset (\Omega \times \mathbb{R}_+)^N$ to provide a wireless communication link to ground terminals (GTs) in a given target region $\Omega \subset \mathbb{R}^d$. Here, the nth UAV's position, $\mathbf{p}_n = (\mathbf{q}_n, h_n)$, is given by its ground position $\mathbf{q}_n = (x_n, y_n) \in \Omega$, representing the quantization point, and its flight height h_n, representing its distortion parameter. The optimal

UAV deployment is then defined by the minimum average communication power (distortion) to serve GTs distributed by a density function λ in Ω with a minimum given data rate R_b. Hereby, each GT will select the UAV which requires the smallest communication power, resulting in so called generalized Voronoi (quantization) regions of Ω, as used in [1]–[3], [5]–[9]. We also assume that the communication between all users and UAVs is orthogonal, i.e., separated in frequency or time (slotted protocols).

In the recent decade, UAVs with directional antennas have been widely studied in the literature [10]–[15], to increase the efficiency of wireless links. However, in [10]–[15], the antenna gain was approximated by a constant within a 3dB beamwidth and set to zero outside. This ignores the strong angle-dependent gain of directional antennas, notably for low-altitude UAVs. To obtain a more realistic model, we will consider an antenna gain which depends on the actual radiation angle $\theta_n \in [0, \frac{\pi}{2}]$ from the nth UAV at $\mathbf{p}_n$ to a GT at $\boldsymbol{\omega}$, see Fig. 1. To capture the power falloff versus the line-of-sight distance d_n along with the random attenuation and the path-loss, we adopt the following propagation model [16, (2.51)]

$$PL_{dB} = 10 \log_{10} K - 10\alpha \log_{10}(d_n/d_0) - \psi_{dB}, \tag{1}$$

where K is a unitless constant depending on the antenna characteristics, d_0 is a reference distance, $\alpha \geq 1$ is the terrestrial path-loss exponent, and ψ_{dB} is a Gaussian random variable following $\mathcal{N}\left(0, \sigma_{\psi_{dB}}^2\right)$. This air-to-ground or terrestrial path-loss model is widely used for UAV basestations path-loss models [17]. Practical values of α are between 2 and 6 and depend on the Euclidean distance of GT $\boldsymbol{\omega}$ and UAV $\mathbf{p}_n$

$$d_n(\boldsymbol{\omega}) = d(\mathbf{p}_n, (\boldsymbol{\omega}, 0)) = \sqrt{\|\mathbf{q}_n - \boldsymbol{\omega}\|^2 + h_n^2} = \sqrt{(x_n - x)^2 + (y_n - y)^2 + h_n^2}. \tag{2}$$

For common practical measurements, see for example [18]. Typically maximal heights for UAVs are < 1000m, due to flight zone restrictions of aircrafts. Hence, the received power at UAV n can be represented as $P_{RX} = P_{TX} G_{TX} G_{RX} K d_0^\alpha d_n^{-\alpha}(\boldsymbol{\omega}) 10^{-\frac{\psi_{dB}}{10}}$, where G_{TX} and G_{RX} are the antenna gains of the transmitter and the receiver, respectively. Here, we assume perfect omnidirectional transmitter GT antennas with an isotropic gain and directional receiver UAV antennas. The angle dependent antenna gains are

$$G_{\text{GT}} > 0 \quad , \quad G_{\text{UAV}} = \cos(\theta_n) = h_n/d_n(\boldsymbol{\omega}), \tag{3}$$

Fig. 1: UAV deployment with directed antenna beam and associated GT cells for $\alpha = 2$ and $N = 2$ for a uniform GT distribution.

see [19, p.52]. The combined antenna intensity is then proportional to $G = G_{\text{UAV}}G_{\text{GT}}K$, see Fig. 1. Accordingly, the received power can be rewritten as

$$P_{RX} = P_{TX}h_n G_{\text{GT}}K d_0^\alpha d_n^{-\alpha-1}(\boldsymbol{\omega})10^{-\frac{\psi_{dB}}{10}}. \tag{4}$$

To achieve a reliable communication between GT and UAV with bit-rate at least R_b for a channel bandwidth B and noise power density N_0, the Shannon formula requires $B \log_2\left(1 + \frac{P_{RX}}{BN_0}\right) \geq R_b$. The minimum transmission power to UAV $\mathbf{p}_n$ is then given by

$$P_{TX} = \left(2^{\frac{R_b}{B}} - 1\right)BN_0 d(\mathbf{p}_n, (\boldsymbol{\omega}, 0))^{\alpha+1}10^{\frac{\psi_{dB}}{10}}(h_n G_{\text{GT}}K d_0^\alpha)^{-1} \tag{5}$$

with expectation

$$\mathbb{E}[P_{TX}] = \frac{(2^{\frac{R_b}{B}} - 1)N_0}{h_n G_{\text{GT}}K d_0^\alpha} \frac{d_n^{\alpha+1}(\boldsymbol{\omega})}{\sqrt{2\pi}\sigma_{\psi_{dB}}} \int_{\mathbb{R}} \exp\left(-\frac{\psi_{dB}^2}{2\sigma_{\psi_{dB}}^2} + \ln(10)\frac{\psi_{dB}}{10}\right)d\psi_{dB} = \frac{\beta}{h_n}d_n^{2\gamma}(\boldsymbol{\omega}) \tag{6}$$

where the independent and fixed parameters are given by

$$\beta = (2^{\frac{R_b}{B}} - 1)BN_0 \exp\left(-\frac{\sigma_{\psi_{dB}}^2(\ln 10)^2}{200}\right)(G_{\text{GT}}K)^{-1}d_0^{-\alpha} \quad \text{and} \quad \gamma = \frac{\alpha+1}{2}. \tag{7}$$

Since our goal is to minimize the average transmission power (6) we define the nth *parameter*

distortion function as

$$D(\boldsymbol{\omega}, \mathbf{q}_n, a_n, b_n) = \beta \cdot \left(a_n \left\| \mathbf{q}_n - \omega \right\|_2^2 + b_n \right)^\gamma \tag{8}$$

where $a_n = h_n^{-1/\gamma}$ and $b_n = h_n^{2-1/\gamma}$. As can be seen from (8), the distortion is a function of the parameter h_n in addition to the distance between the reproduction point $\mathbf{q}_n$ and the represented point $\boldsymbol{\omega}$. From a quantization point of view, one can start with the distortion function (8) without knowing the UAV power consumption formulas in this section. This is what we will do in the next section. For simplicity, we will set from here on $\beta = 1$, since it will not affect the quantizer.

III. Optimizing Quantizers with parameterized distortion measures

The communication power cost (8) defines, with h_n and fixed $\gamma \geq 1$, a parameter-dependent distortion function for $\mathbf{q}_n$. For a given source sample GT density λ in Ω and UAV deployment, the average power is the average distortion for given *quantization and parameter points* $(\mathbf{Q}, \mathbf{h})$ with quantization sets $\mathcal{R} = \{\mathcal{R}_n\}$, which is called the *average distortion* of the quantizer $(\mathbf{Q}, \mathbf{h}, \mathcal{R})$

$$\bar{D}(\mathbf{Q}, \mathbf{h}, \mathcal{R}) = \sum_{n=1}^{N} \int_{\mathcal{R}_n} D(\boldsymbol{\omega}, \mathbf{q}_n, h_n) \lambda(\boldsymbol{\omega}) d\boldsymbol{\omega}. \tag{9}$$

The N quantization sets, which minimize the average distortion for given quantization and parameter points $(\mathbf{Q}, \mathbf{h})$, define a generalized Voronoi tessellation $\mathcal{V} = \{\mathcal{V}_n(\mathbf{Q}, \mathbf{h})\}$

$$\bar{D}(\mathbf{Q}, \mathbf{h}, \mathcal{V}) := \int_{\Omega} \min_{n \in [N]} \left\{ D(\boldsymbol{\omega}, \mathbf{q}_n, h_n) \right\} \lambda(\boldsymbol{\omega}) d\boldsymbol{\omega} = \sum_{n=1}^{N} \int_{\mathcal{V}_n(\mathbf{Q}, \mathbf{h})} D(\boldsymbol{\omega}, \mathbf{q}_n, h_n) \lambda(\boldsymbol{\omega}) d\boldsymbol{\omega}, \tag{10}$$

where the *generalized Voronoi regions* $\mathcal{V}_n(\mathbf{Q}, \mathbf{h})$ are defined as the set of sample points $\boldsymbol{\omega}$ with smallest distortion to the nth quantization point $\mathbf{q}_n$ with parameter h_n. Minimizing the *average distortion* $\bar{D}(\mathbf{Q}, \mathbf{h}, \mathcal{V})$ over all parameter and quantization points can be seen as an $N-$*facility locational-parameter optimization problem* [5]–[7], [20]. By the definition of the Voronoi regions (10), this is equivalent to the minimum average distortion over all $N-$level parameter quantizers

$$\bar{D}(\mathbf{Q}^*, \mathbf{h}^*, \mathcal{V}^*) = \min_{(\mathbf{Q}, \mathbf{h}) \in \Omega^N \times \mathbb{R}_+^N} \bar{D}(\mathbf{Q}, \mathbf{h}, \mathcal{V}) = \min_{(\mathbf{Q}, \mathbf{h}) \in \Omega^N \times \mathbb{R}_+^N} \min_{\mathcal{R} = \{\mathcal{R}_n\} \subset \Omega} \bar{D}(\mathbf{Q}, \mathbf{h}, \mathcal{R}), \tag{11}$$

which we call the $N-$*level parameter optimized quantizer*. To find local extrema of (10) analytically, we will need that the objective function $\bar{D}$ be continuously differentiable at any point in $\Omega^N \times \mathbb{R}_+^N$, i.e., the gradient should exist and be a continuous function. Such a property was shown to be true for piecewise continuous non-decreasing distortion functions in the Euclidean

metric over Ω^N [21, Thm.2.2] and weighted Euclidean metric [5]. Then the necessary condition for a local extremum is the vanishing of the gradient at a critical point[1]. First, we will derive the generalized Voronoi regions for convex sets Ω in d dimensions for any parameters $h_n \in \mathbb{R}_+$ for the quantization points $\mathbf{q}_n$, which are special cases of *Möbius diagrams (tessellations)*, introduced in [4].

Lemma 1. *Let* $\mathbf{Q} = \{\mathbf{q}_1, \mathbf{q}_2, \ldots, \mathbf{q}_N\} \subset \Omega^N \subset (\mathbb{R}^d)^N$ *for* $d \in \{1, 2\}$ *be the quantization points and* $\mathbf{h} = (h_1, \ldots, h_N) \in \mathbb{R}_+^N$ *the associated parameters. Then the average distortion of* $(\mathbf{Q}, \mathbf{h})$ *over all samples in* Ω *distributed by* λ *for some exponent* $\gamma \geq 1$

$$\bar{D}(\mathbf{Q}, \mathbf{h}, \mathcal{V}) = \sum_{n=1}^{N} \int_{\mathcal{V}_n} \frac{(\|\mathbf{q}_n - \boldsymbol{\omega}\|^2 + h_n^2)^\gamma}{h_n} \lambda(\boldsymbol{\omega}) d\boldsymbol{\omega} \tag{12}$$

has generalized Voronoi regions $\mathcal{V}_n = \mathcal{V}_n(\mathbf{Q}, \mathbf{h}) = \bigcap_{m \neq n} \mathcal{V}_{nm}$, *where the dominance regions of quantization point* n *over* m *are given by*

$$\mathcal{V}_{nm} = \Omega \cap \begin{cases} \mathcal{H}(\mathbf{q}_n, \mathbf{q}_m) & , h_m = h_n \\ B(\mathbf{c}_{nm}, r_{nm}) & , h_n < h_m \\ B^c(\mathbf{c}_{nm}, r_{nm}) & , h_n > h_m \end{cases} \tag{13}$$

and center and radii of the balls are given by

$$\mathbf{c}_{nm} = \frac{\mathbf{q}_n - h_{nm}\mathbf{q}_m}{1 - h_{nm}} \quad and \quad r_{nm} = \left(\frac{h_{nm}}{(1 - h_{nm})^2} \|\mathbf{q}_n - \mathbf{q}_m\|^2 + h_n^2 \frac{h_{nm}^{1-2\gamma} - 1}{1 - h_{nm}} \right)^{\frac{1}{2}}. \tag{14}$$

Here, we introduced the parameter ratio of the nth *and* mth *quantization point as*

$$h_{nm} = (h_n / h_m)^{\frac{1}{\gamma}}. \tag{15}$$

Remark. It is also possible that two quantization points are equal, but have different parameters. If the parameter ratio is very small or very large, one quantization point can become redundant, i.e., if its optimal quantization set is empty. In fact, if we optimize over all quantizer points, such a case will be excluded, which we will show for one-dimension in Lemma 3.

Proof. The minimization of the distortion functions over Ω defines an assignment rule for a

---

[1]Note, if $\nabla \bar{P}$ is not continuous in $\mathcal{P}^N$ than any jump-point is a potential critical point and has to be checked individually.

generalized Voronoi diagram $\mathcal{V}(\mathbf{Q}, \mathbf{h}) = \{\mathcal{V}_1, \mathcal{V}_2, \ldots, \mathcal{V}_N\}$ where

$$\mathcal{V}_n = \mathcal{V}_n(\mathbf{Q}, \mathbf{h}) := \left\{ \boldsymbol{\omega} \in \Omega \mid a_n \left\| \mathbf{q}_n - \boldsymbol{\omega} \right\|^2 + b_n \leq a_m \left\| \mathbf{q}_m - \boldsymbol{\omega} \right\|^2 + b_m, m \neq n \right\} \qquad (16)$$

is the nth generalized Voronoi region, see for example [20, Cha.3]. Here we denoted the weights by the positive numbers

$$a_n = h_n^{-\frac{1}{\gamma}}, \quad b_n = h_n^{2-\frac{1}{\gamma}} \qquad (17)$$

which define a *Möbius diagram* [4], [22]. The bisectors of Möbius diagrams are circles or lines in $\mathbb{R}^2$ as we will show below. The nth Voronoi region is defined by $N - 1$ inequalities, which can be written as the intersection of the $N - 1$ *dominance regions* of $\mathbf{q}_n$ over $\mathbf{q}_m$, given by

$$\mathcal{V}_{nm} = \left\{ \boldsymbol{\omega} \in \Omega \mid a_n \left\| \mathbf{q}_n - \boldsymbol{\omega} \right\|^2 + b_n \leq a_m \left\| \mathbf{q}_m - \boldsymbol{\omega} \right\|^2 + b_m \right\}. \qquad (18)$$

If $h_n = h_m$ then $a_n = a_m$ and $b_n = b_m$, such that $\mathcal{V}_{nm} = \mathcal{H}(\mathbf{q}_n, \mathbf{q}_m)$, the left half-space between $\mathbf{q}_n$ and $\mathbf{q}_m$. For $a_n > a_m$ we can rewrite the inequality as

$$\left\| \boldsymbol{\omega} \right\|^2 - 2 \left\langle \mathbf{c}_{nm}, \boldsymbol{\omega} \right\rangle + \frac{a_n^2 \left\| \mathbf{q}_n \right\|^2 + a_m^2 \left\| \mathbf{q}_m \right\|^2 - a_n a_m (\left\| \mathbf{q}_n \right\|^2 + \left\| \mathbf{q}_m \right\|^2)}{(a_n - a_m)^2} + \frac{b_n - b_m}{a_n - a_m} \leq 0$$

where the center point is given by

$$\mathbf{c}_{nm} = \frac{a_n \mathbf{q}_n - a_m \mathbf{q}_m}{a_n - a_m} = a_n \frac{\mathbf{q}_n - h_{nm} \mathbf{q}_m}{a_n - a_m} = \frac{\mathbf{q}_n - h_{nm} \mathbf{q}_m}{1 - h_{nm}} \qquad (19)$$

where we introduced the *parameter ratio* of the nth and mth quantization point as

$$h_{nm} := a_m / a_n = (h_n / h_m)^{\frac{1}{\gamma}} > 0. \qquad (20)$$

If $0 < a_n - a_m$, which is equivalent to $h_n < h_m$, then this defines a ball (disc) and for $h_n > h_m$ its complement. Hence we get

$$\mathcal{V}_{nm} = \begin{cases} B(\mathbf{c}_{nm}, r_{nm}) = \left\{ \boldsymbol{\omega} \in \Omega \mid \left\| \boldsymbol{\omega} - \mathbf{c}_{nm} \right\| < r_{nm} \right\}, & h_n < h_m \\ \mathcal{H}(\mathbf{q}_n, \mathbf{q}_m) = \left\{ \boldsymbol{\omega} \in \Omega \mid \left\| \boldsymbol{\omega} - \mathbf{q}_n \right\| \leq \left\| \boldsymbol{\omega} - \mathbf{q}_m \right\| \right\}, & h_n = h_m \\ B^c(\mathbf{c}_{nm}, r_{nm}) = \left\{ \boldsymbol{\omega} \in \Omega \mid \left\| \boldsymbol{\omega} - \mathbf{c}_{nm} \right\| > r_{nm} \right\}, & h_n > h_m \end{cases} \qquad (21)$$

where the radius square is given by

$$r_{nm}^2 = a_n a_m \frac{\|\mathbf{q}_n - \mathbf{q}_m\|^2}{(a_n - a_m)^2} + \frac{b_m - b_n}{a_n - a_m} = \frac{a_n}{a_m} \frac{\|\mathbf{q}_n - \mathbf{q}_m\|^2}{(1 - \frac{a_n}{a_m})^2} + \frac{b_m - b_n}{a_n - a_m}. \tag{22}$$

The second summand can be written as

$$\frac{b_m - b_n}{a_n - a_m} = \frac{h_m^{2-\frac{1}{\gamma}} - h_n^{2-\frac{1}{\gamma}}}{h_n^{-\frac{1}{\gamma}} - h_m^{-\frac{1}{\gamma}}} = \frac{h_n^2 \left((h_n/h_m)^{\frac{1}{\gamma} - 2} - 1 \right)}{1 - (h_n/h_m)^{\frac{1}{\gamma}}} = h_n^2 \frac{h_{nm}^{-\alpha} - 1}{1 - h_{nm}}. \tag{23}$$

For any $\gamma \geq 1$, we have $h_{nm} = (h_n/h_m)^{1/\gamma} < 1$ if $h_n < h_m$ and $h_{nm} \geq 1$ else. In both cases (23) is positive, which implies a radius $r_{nm} > 0$ whenever $\mathbf{q}_n \neq \mathbf{q}_m$. Inserting (23) in (22) yields the result. ∎

Example 1. We plotted in Fig. 1, for $N = 2$ and $\Omega = [0,1]^2$, the GT regions for a uniform distribution with UAVs placed on

$$\mathbf{q}_1 = (0.1, 0.2), h_1 = 0.5, \quad \text{and} \quad \mathbf{q}_2 = (0.6, 0.6), h_2 = 1. \tag{24}$$

If the second UAV reaches an altitude of $h_2 \geq 2.3$, its Voronoi region $\mathcal{V}_2 = \mathcal{V}_{2,1}$ will be empty and hence become "inactive".

A. Local optimality conditions

To find the optimal $N-$level parameter quantizer (10), we have to minimize the average distortion (9) over all possible quantization-parameter points, i.e., we have to solve a non-convex $N-$*facility locational-parameter optimization problem*,

$$\bar{D}(\mathbf{Q}^*, \mathbf{h}^*, \mathcal{V}^*) = \min_{\mathbf{Q} \in \Omega^N, \mathbf{h} \in \mathbb{R}_+^N} \sum_{n=1}^{N} \int_{\mathcal{V}_n(\mathbf{Q}, \mathbf{h})} h_n^{-1}(\|\mathbf{q}_n - \boldsymbol{\omega}\|^2 + h_n^2)^\gamma \lambda(\boldsymbol{\omega}) d\boldsymbol{\omega} \tag{25}$$

where $\mathcal{V}_n(\mathbf{Q}, \mathbf{h})$ are the Möbius regions given in (13) for each fixed $(\mathbf{Q}, \mathbf{h})$. A point $(\mathbf{Q}^*, \mathbf{h}^*)$ with Möbius diagram $\mathcal{V}^* = \mathcal{V}(\mathbf{Q}^*, \mathbf{h}^*) = \{\mathcal{V}_1^*, \ldots, \mathcal{V}_N^*\}$ is a critical point of (25) if all partial derivatives of $\bar{D}$ are vanishing, i.e., if for each $n \in [N]$ it holds

$$0 = \int_{\mathcal{V}_n^*} (\mathbf{q}_n^* - \boldsymbol{\omega})(\|\mathbf{q}_n^* - \boldsymbol{\omega}\|^2 + h_n^{*2})^{\gamma-1} \lambda(\boldsymbol{\omega}) d\boldsymbol{\omega} \tag{26}$$

$$0 = \int_{\mathcal{V}_n^*} (\|\mathbf{q}_n^* - \boldsymbol{\omega}\|^2 + h_n^{*2})^{\gamma-1} \cdot (\|\mathbf{q}_n^* - \boldsymbol{\omega}\|^2 - (2\gamma - 1)h_n^{*2}) \lambda(\boldsymbol{\omega}) d\boldsymbol{\omega}. \tag{27}$$

For $N = 1$ the integral regions will not depend on $\mathbf{Q}$ or $\mathbf{h}$ and since the integral kernel is continuous differentiable, the partial derivatives will only apply to the integral kernel. For $N > 1$, the conservation-of-mass law, can be used to show that the derivatives of the integral domains will cancel each other out, see also [21].

Remark. The shape of the regions depend on the parameters, which if different for each quantization point (heterogeneous), generate spherical and not polyhedral regions. We will show later, that homogeneous parameter selection with polyhedral regions will be the optimal regions for $d = 1$.

B. The optimal $N-$level parameter quantizer in one-dimension for uniform density

In this section, we discuss the parameter optimized quantizer for a one-dimensional convex source $\Omega \subset \mathbb{R}$, i.e., for an interval $\Omega = [s, t]$ given by some real numbers $s < t$. Under such circumstances, the quantization points are degenerated to scalars, i.e., $\mathbf{q}_n = x_n \in [s, t], \ \forall \ n \in [N]$. If we shift the interval Ω by an arbitrary $a \in \mathbb{R}$, then the average distortion, i.e., the objective function, will not change if we shift all quantization points by the same number a. Hence, if we set $a = -s$, we can shift any quantizer for $[s, t]$ to $[0, A]$ where $A = t - s$ without loss of generality. Let us assume a uniform distribution on Ω, i.e. $\lambda(\omega) = 1/A$. To derive the unique $N-$level parameter optimized quantizer for any N, we will first investigate the case $N = 1$.

Lemma 2. *Let $A > 0$ and $\gamma \geq 1$. The unique $1-$level parameter optimized quantizer (x^*, h^*) with distortion function (8) is given for a uniform source density in $[0, A]$ by*

$$x^* = \frac{A}{2}, h^* = \frac{A}{2}g(\gamma) \quad \text{and the minimum average distortion} \quad \bar{D}(x^*, h^*) = \left(\frac{A}{2}\right)^{2\gamma - 1}g(\gamma)$$

where $g(\gamma) = \arg\min_{u>0} F(u, \gamma) < 1/\sqrt{2\gamma - 1}$ is the unique minimizer of

$$F(u, \gamma) = \int_0^1 f(\omega, u, \gamma)d\omega \quad \text{with} \quad f(\omega, u, \gamma) = \frac{(\omega^2 + u^2)^\gamma}{u} \tag{28}$$

which is for fixed γ a continuous and convex function over $\mathbb{R}_+$. For $\gamma \in \{1, 2, 3\}$ the minimizer can be derived in closed form as

$$g(1) = \sqrt{1/3}, \quad g(2) = \sqrt{(\sqrt{32/5} - 1)/9}, \quad g(3) = \sqrt{\left((32/7)^{1/3} - 1\right)/5}. \tag{29}$$

Proof. See Appendix A. ∎

Remark. The convexity of $F(\cdot, \gamma)$ can be also shown by using extensions of the Hermite-Hadamard inequality [23], which allows to show convexity over any interval. Let us note here that for any fixed parameter $h_n > 0$, the average distortion $\bar{D}(x_n^* \pm \epsilon, h_n)$ is strictly monotone increasing in $\epsilon > 0$. Hence, x_n^* is the unique minimizer for any $h_n > 0$. We will use this decoupling property repeatedly in the proofs [24].

To derive our main result, we need some general properties of the optimal regions.

Lemma 3. *Let* $\Omega = [0, A]$ *for some* $A > 0$. *The* $N-$*level parameter optimized quantizer* $(\mathbf{Q}^*, \mathbf{h}^*) \in \Omega^N \times \mathbb{R}_+^N$ *for a uniform source density in* Ω *has optimal quantization regions* $\mathcal{V}_n(\mathbf{Q}^*, \mathbf{h}^*) = [b_{n-1}^*, b_n^*]$ *with* $0 \leq b_{n-1}^* < b_n^* \leq A$ *and optimal quantization points* $x_n^* = (b_n^* + b_{n-1}^*)/2$ *for* $n \in [N]$, *i.e., each region is a closed interval with positive measure and centroidal quantization points.*

Proof. See Appendix B. ∎

Remark. Hence, for an $N-$level parameter optimized quantizer, all quantization points are used, which is intuitively, since each additional quantization point should reduce the distortion of the quantizer by partitioning the source in non-zero regions.

Theorem 1. *Let* $N \in \mathbb{N}$, $\Omega = [0, A]$ *for some* $A > 0$, *and* $\gamma \geq 1$. *The* unique $N-$level parameter optimized quantizer $(\mathbf{Q}^*, \mathbf{h}^*, \mathcal{R}^*)$ *is the uniform scalar quantizer with identical parameter values, given for* $n \in [N]$ *by*

$$\mathbf{q}_n^* = x_n^* = \frac{A}{2N}(2n - 1), \quad h^* = h_n^* = \frac{A}{2N}g(\gamma), \quad \mathcal{R}_n^* = \left[\frac{A}{N}(n-1), \frac{A}{N}n\right] \tag{30}$$

with minimum average distortion

$$\bar{D}(\mathbf{Q}^*, \mathbf{h}^*, \mathcal{R}^*) = \left(\frac{A}{2N}\right)^{2\gamma - 1} \int_0^1 \frac{\left(\omega^2 + g^2(\gamma)\right)^{\gamma}}{g(\gamma)} d\omega. \tag{31}$$

For $\gamma \in \{1, 2, 3\}$, *the closed form* $g(\gamma)$ *is provided in* (29).

Proof. See Appendix C. ∎

Example 2. We plot the optimal heights and optimal average distortion for a uniform GT density in $[0, 1]$ over various α and $N = 2$ in Fig. 2. Note that the factor $A/2N = 1/4$ will play a crucial
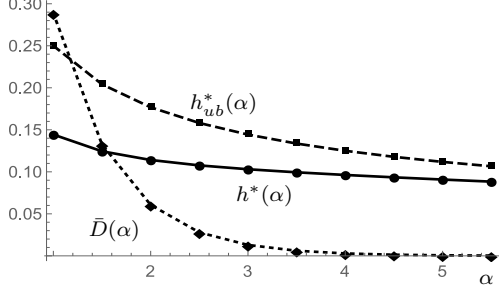
Fig. 2: Optimal height (solid) with bound (dashed) and average distortion (dotted) for $N = 2, A = 1$ and uniform GT density.
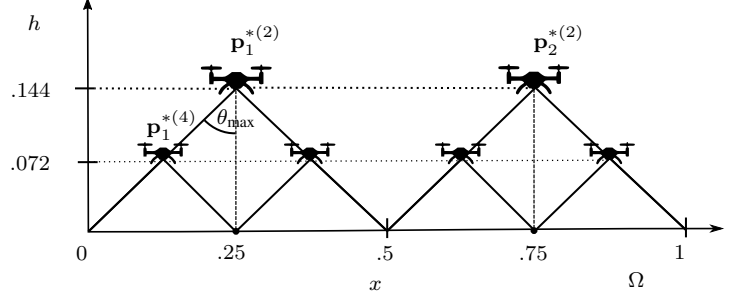

Fig. 3: Optimal UAV deployment in one dimension for $A = 1, \alpha = 1$ and $N = 2, 4$ over a uniform GT density by (30).

role for the height and distortion scaling. Moreover, the distortion decreases exponentially in α if $A/2N < 1$.

Let us set $\beta = 1 = A$. Then, the optimal UAV deployment is pictured in Fig. 3 for $N = 2$ and $N = 4$. The maximum elevation angle $\theta_{\max}$ is hereby constant for each UAV and does not change if the number of UAVs, N, increases. Moreover, it is also independent of A and β, since with (30) we have $\mu_n^* = x_n^* - x_{n-1}^* = A/N$ and

$$\cos(\theta_{\max}) = \cos(\theta_n) = \frac{h^*}{\mu_n^*/2} = \frac{2N}{A} \frac{A}{2N} g(1) = \frac{1}{\sqrt{3}}. \tag{32}$$

IV. LLYOD-LIKE ALGORITHMS AND SIMULATION RESULTS

In this section, we introduce two Lloyd-like algorithms, Lloyd-A and Lloyd-B, to optimize the quantizer for two-dimensional scenarios. The proposed algorithms iterate between two steps: (1) The reproduction points are optimized through gradient descent while the partitioning is fixed; (ii) The partitioning is optimized while the reproduction points are fixed. In Lloyd-A, all UAVs (or reproduction points) share the common flight height while Lloyd-B allows UAVs at different flight heights.

In what follows, we provide the simulation results over the two-dimensional target region $\Omega = [0, 10]^2$ with uniform and non-uniform density functions. The non-uniform density function is a Gaussian mixture of the form $\sum_{k=1}^3 \frac{A_k}{\sqrt{2\pi\sigma_k^2}} \exp\left(-\frac{\|\omega - c_k\|^2}{2\sigma_k}\right)$, where the weights, A_k, $k = 1, 2, 3$ are $0.5, 0.25, 0.25$, the means, c_k, are $(3, 3), (6, 7), (7.5, 2.5)$, the standard deviations, σ_k, are $1.5, 1$, and 2, respectively.
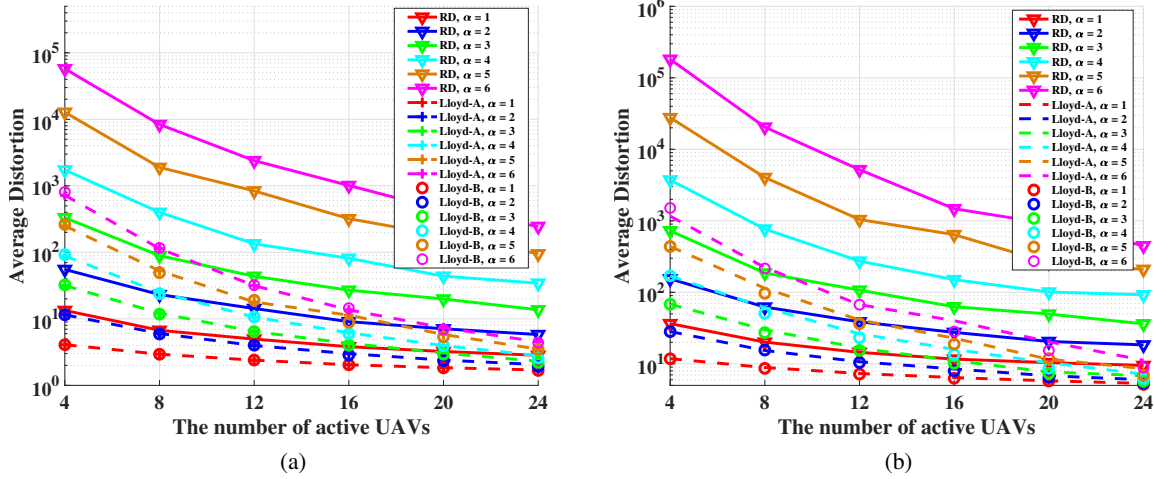
Fig. 4: The performance comparison of Lloyd-A, Lloyd-B and Random Deployment (RD). (a) Uniform density. (b) Non-uniform density.

To evaluate the performance of the proposed algorithms, we compare them with the average distortion of 100 random deployments (RDs). Figs. 4a and 4b, show that the proposed algorithms outperform the random deployment on both uniform and non-uniform distributed target regions. From Fig. 4a, one can also find that the distortion achieved by Lloyd-A and Lloyd-B are very close, indicating that the optimality of the common height, as proved for the one-dimensional case in Section III, might be extended to the two-dimensional case when the density function is uniform. However, one can find a non-negligible gap between Lloyd-A and Lloyd-B in Fig. 4b where the density function is non-uniform. For instance, given 16 UAVs and the path-loss exponent $\alpha = 6$, Lloyd-A's distortion is 40.17 while Lloyd-B obtains a smaller distortion, 28.25, by placing UAVs at different heights. Figs. 5a and 5b illustrate the UAV ground projections and their partitions on a uniform distributed square region. As the number of UAVs increases, the UAV partitions approximate hexagons which implies that the optimality of congruent partition (Theorem 1) might be extended to uniformly distributed users for two-dimensional sources. However, the UAV projections in Figs. 6a and 6b show that congruent partition is no longer a necessary condition for the optimal quantizer when distribution is non-uniform.

V. CONCLUSION

We studied quantizers with parameterized distortion measures for an application to UAV deployments. Instead of using the traditional mean distance square as the distortion, we introduce a distortion function which models the energy consumption of UAVs in dependence of their
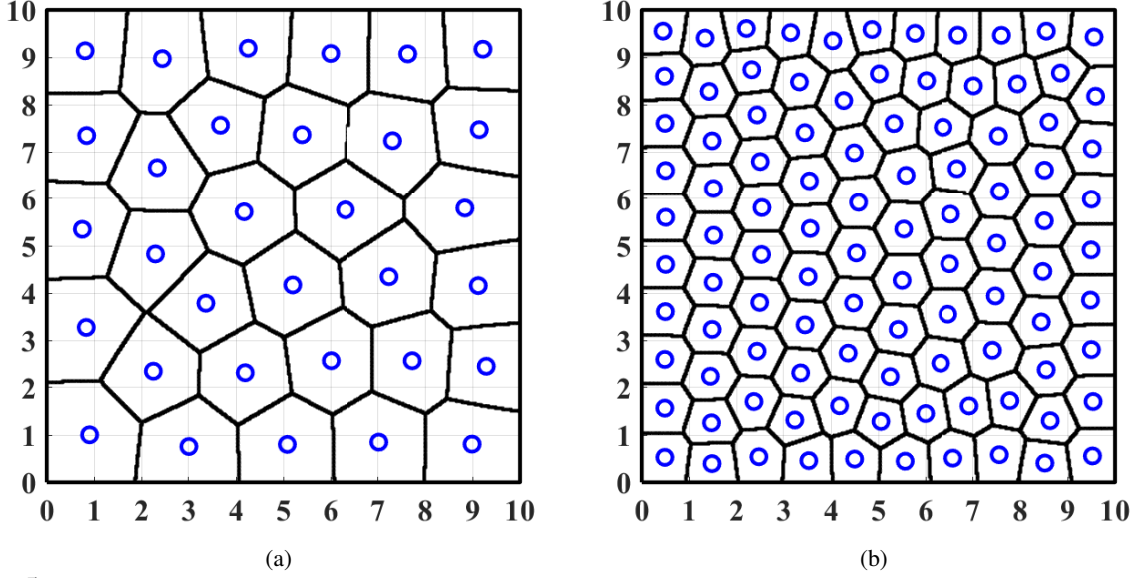
Fig. 5: The UAV projections on the ground with generalized Voronoi Diagrams where $\alpha = 2$ and the source distribution is uniform. (a) 32 UAVs. (b) 100 UAVs.
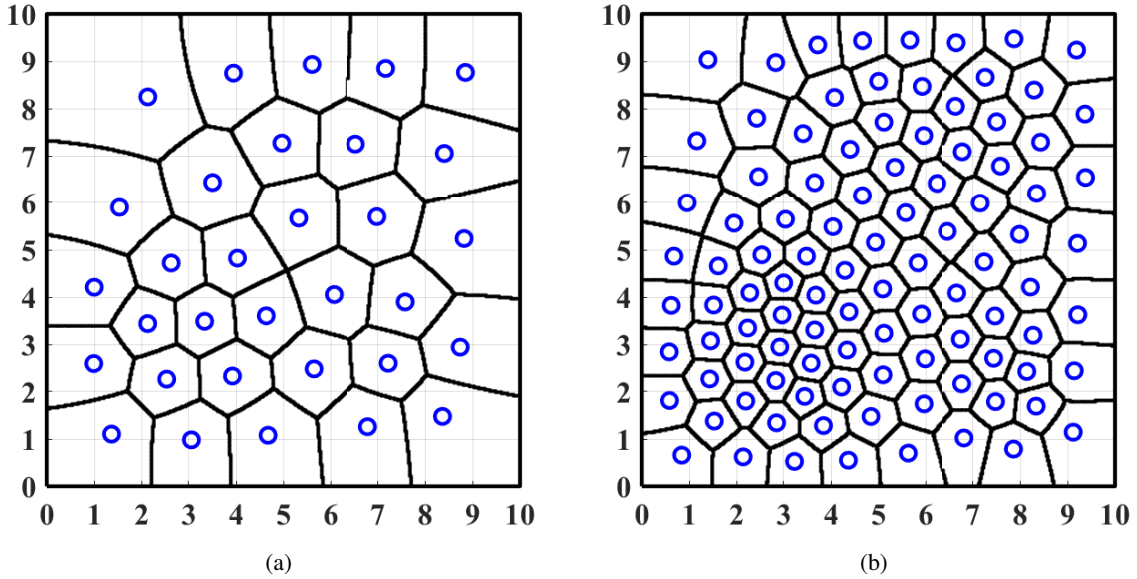

Fig. 6: The UAV projections on the ground with generalized Voronoi Diagrams where $\alpha = 2$ and the source distribution is non-uniform. (a) 32 UAVs. (b) 100 UAVs.

heights. We derived the unique parameter optimized quantizer – a uniform scalar quantizer with an optimal common parameter – for uniform source density in one-dimensional space. In addition, two Lloyd-like algorithms are designed to minimize the distortion in two-dimensional space. Numerical simulations demonstrate that the common weight property extends to two-dimensional space for a uniform density.

APPENDIX A

PROOF OF LEMMA 2

To find the optimal $1-$level parameter quantizer (x^*, h^*) for a uniform density $\lambda(\omega) = 1/A$, we need to satisfy (27), i.e., for[2] $\Omega = \mathcal{V}_1 = \mathcal{V}_1^* = [0, A]$

$$0 = \int_0^A (x^* - \omega)\big((x^* - \omega)^2 + h^{*2}\big)^{\gamma - 1} d\omega. \tag{33}$$

Substituting $x^* - \omega$ by ω we get

$$0 = \int_{x^* - A}^{x^*} \omega\big(\omega^2 + h^{*2}\big)^{\gamma - 1} d\omega. \tag{34}$$

Since the integral kernel is an odd function in ω and $x^* \in [0, A]$, it must hold

$$0 = -\int_0^{x^* - A} \omega(\omega^2 + h^{*2})^{\gamma - 1} d\omega + \int_0^{x^*} \omega(\omega^2 + h^{*2})^{\gamma - 1} d\omega \tag{35}$$

by substituting ω by $-\omega$ we get

$$\int_0^{A - x^*} \omega(\omega^2 + h^{*2})^{\gamma - 1} d\omega = \int_0^{x^*} \omega(\omega^2 + h^{*2})^{\gamma - 1} d\omega. \tag{36}$$

Hence for any choice of h^* it must hold $x^* = A - x^*$, which is equivalent to $x^* = A/2$. To find the optimal parameter, we can just insert x^* into the average distortion

$$\bar{D}(x^*, h) = \frac{1}{A} \int_0^A \frac{(x^* - \omega)^2 + h^2)^\gamma}{h} d\omega = \frac{1}{A} \int_0^{A/2} \frac{(\omega^2 + h^2)^\gamma}{h} d\omega \tag{37}$$

where we substituted again and inserted $x^* = A/2$. By substituting ω with $2\omega/A$ and h with $u = 2h/A$ we get

$$= \int_0^1 \frac{2}{A} \frac{((A\omega/2)^2 + (Au/2)^2)^\gamma}{u} d\omega = \left(\frac{A}{2}\right)^{2\gamma - 1} \int_0^1 f(\omega, u, \gamma) d\omega \tag{38}$$

where for each $\gamma \geq 1$ the integral kernel f is a convex function in $\mathbf{x} = (\omega, u)$ over $\mathbb{R}_+^2$. Let us rewrite f as

$$f(\omega, u, \gamma) = \frac{(\omega^2 + u^2)^\gamma}{u} = \frac{\|(\omega, u)\|_2^{2\gamma}}{u}. \tag{39}$$

Clearly, $\|\mathbf{x}\|_2$ is a convex and continuous function in $\mathbf{x}$ over $\mathbb{R}^2$ and since $(\cdot)^{2\gamma}$ with $2\gamma \geq 2$ is a strictly increasing continuous function, the concatenation $f(\mathbf{x}, \gamma)$ is a strict convex and

---

[2]Note, there is no optimizing over the regions, since there is only one.

continuous function over $\mathbb{R}_+^2$. Hence, for any $\mathbf{x}_1, \mathbf{x}_2 \in \mathbb{R}^2$ we have

$$\|\lambda \mathbf{x}_1 + (1-\lambda)\mathbf{x}_2\|_2^{2\gamma} < \lambda \|\mathbf{x}_1\|_2^{2\gamma} + (1-\lambda)\|\mathbf{x}_2\|_2^{2\gamma} \tag{40}$$

for all $\lambda \in (0,1)$. But then we have also for any $u_1, u_2 \in \mathbb{R}_+^2$ and $\omega \geq 0$

$$f(\lambda u_1 + (1-\lambda)u_2, \omega, \gamma) < \frac{\lambda \|(\omega, u_1)\|_2^{2\gamma} + (1-\lambda)\|(\omega, u_2)\|_2^{2\gamma}}{\lambda u_1 + (1-\lambda)u_2}. \tag{41}$$

Considering the following inequality

$$\frac{1}{u_1} + \frac{1}{u_2} = \left(\frac{1}{u_1} + \frac{1}{u_2}\right) \frac{\lambda u_1 + (1-\lambda)u_2}{\lambda u_1 + (1-\lambda)u_2} = \frac{\left(\lambda + \frac{(1-\lambda)u_2}{u_1} + (1-\lambda) + \frac{\lambda u_1}{u_2}\right)}{\lambda u_1 + (1-\lambda)u_2} > \frac{1}{\lambda u_1 + (1-\lambda)u_2}$$

and (41), we will have

$$f(\lambda u_1 + (1-\lambda)u_2, \omega, \gamma) < \lambda f(u_1, \omega, \gamma) + (1-\lambda)f(u_2, \omega, \gamma) \tag{42}$$

for every $\lambda \in (0,1)$. Hence, the integral kernel is a strictly convex function for every $\omega \geq 0, \gamma \geq 1$, and since the infinite sum (integral) of convex functions is again a convex function, for $u > 0$, we have shown convexity of $F(u, \gamma)$. Note, $f(u, \omega, \gamma)$ is continuous in $\mathbb{R}_+^2$ since it is a product of the continuous functions $\|(u, \omega)\|_2^{2\gamma}$ and $1/(u + 0 \cdot \omega)$, and so is $F(u, \gamma)$. Therefore, the only critical point of $F(\cdot, \gamma)$ will be the unique global minimizer

$$g(\gamma) = \arg\min_{u > 0} F(u, \gamma), \tag{43}$$

which is defined by the vanishing of the first derivative:

$$F'(u) = \int_0^1 (\omega^2 + u^2)^{\gamma-1} \left((2\gamma - 1) - \frac{\omega^2}{u^2}\right) d\omega = \frac{1}{u^2} \int_0^1 (\omega^2 + u^2)^{\gamma-1} \left((2\gamma - 1)u^2 - \omega^2\right) d\omega. \tag{44}$$

Hence, $F'(u)$ can only vanish if $u < 1/\sqrt{2\gamma - 1}$, which is an upper bound on $g(\gamma)$. The optimal parameter for minimizing the average distortion (37) is then

$$h^* = \frac{A}{2} g(\gamma) \quad \text{with} \quad \bar{D}(x^*, h^*) = \left(\frac{A}{2}\right)^{2\gamma-1} g(\gamma). \tag{45}$$

Analytical solutions for $F'(u) = 0$ are possible for integer valued γ. Let us set $0 < x = u^2$ in (44), then for $\gamma \in \mathbb{N}$, the integrand in (44) will be a polynomial in ω of degree 2γ and in x of

degree γ. For $\gamma \in \{1, 2, 3\}$ the integrand will be

$$(\omega^2 + x)^0(1x - \omega^2) = x - \omega^2 \tag{46}$$

$$(\omega^2 + x)^1(3x - \omega^2) = 3x^2 + 2\omega^2 x - \omega^4 \tag{47}$$

$$(\omega^2 + x)^2(5x - \omega^2) = 5x^3 + 9\omega^2 x^2 + 3\omega^4 x - \omega^6 \tag{48}$$

which yield with the definite integrals to

$$0 = \omega(x - \frac{\omega^2}{3})\Big|_{\omega=1} \tag{49}$$

$$0 = \omega(3x^2 + \frac{2\omega^2 x}{3} - \frac{\omega^4}{5})\Big|_{\omega=1} \tag{50}$$

$$0 = \omega(5x^3 + 3\omega^2 x^2 + \frac{3\omega^4 x}{5} - \frac{\omega^6}{7})\Big|_{\omega=1} \tag{51}$$

Solving (49) for x yields to the only feasible solution

$$x = \frac{1}{3} \quad \Rightarrow \quad g(1) = \frac{1}{\sqrt{3}} \approx 0.577. \tag{52}$$

The solutions of (50) are

$$x_{\pm} = -\frac{1}{9} \pm \sqrt{\frac{1}{81} + \frac{1}{15}} = \frac{\pm\sqrt{32/5} - 1}{9} \tag{53}$$

Since only positive roots are allowed, we get as the only feasible solution

$$g(3) = \frac{\sqrt{\sqrt{32/5} - 1}}{3} \approx 0.412. \tag{54}$$

Finally, the cubic equation (51) results in

$$5x^3 + 3x^2 + \frac{3}{5}x - \frac{1}{7} = 0 \tag{55}$$

The solution of a cubic equation can be found in [25, p. 2.3.2] by calculating the discriminant

$$\Delta = q^2 + 4p^3 \quad \text{with} \quad q = \frac{2b^3 - 9abc + 27a^2 d}{27a^3}, p = \frac{3ac - b^2}{9a^2} \tag{56}$$

Let us identify $a = 5, b = 3, c = 3/5$ and $d = -1/7$, then we get

$$q = \frac{6 \cdot 9 - 9 \cdot 9 - 27 \cdot 5^2 \cdot 1/7}{27 \cdot 5^3} = -\frac{3}{3 \cdot 5 \cdot 25} - \frac{1}{5 \cdot 7} = -\frac{32}{25 \cdot 35} \tag{57}$$

$$\Delta = q^2 + 4 \left(\frac{3 \cdot 3 - 9}{9 \cdot 5^2} \right)^3 = q^2 > 0 \tag{58}$$

which indicates only one real-valued root, given by

$$x = \alpha_+^{1/3} + \alpha_-^{1/3} - \frac{b}{3a} \quad \text{with} \quad \alpha_\pm = \frac{-q \pm \sqrt{\Delta}}{2} = \left\{ 0, \frac{32}{25 \cdot 35} \right\} \tag{59}$$

which computes to

$$x = \left(\frac{32}{5^3 \cdot 7} \right)^{1/3} - \frac{1}{5} = \frac{(\frac{32}{7})^{1/3} - 1}{5} \Rightarrow g(5) = \sqrt{\frac{(\frac{32}{7})^{1/3} - 1}{5}} \approx 0.363. \tag{60}$$

APPENDIX B

PROOF OF LEMMA 3

Although, this statement seems to be trivial, it is not straight forward to show. We will use the quantization relaxation for the average distortion $\bar{D}$ in (9) to show that the $N-$level parameter optimized quantizer has strictly smaller distortion than the $(N - 1)-$level optimized quantizer (10). We define, as in quantization theory, see for example [26], an $N-level$ $quantizer$ for Ω, by a (disjoint) partition $\mathcal{R} = \{\mathcal{R}_n\}_{n=1}^N \subset \Omega$ of Ω and assign to each partition region $\mathcal{R}_n$ a quantization-parameter point $(\mathbf{q}_n, h_n) \in \Omega \times \mathbb{R}_+$. The assignment rule or *quantization rule* can be anything such that the regions are independent of the value of the quantization and parameter points. Minimizing over the quantizer, that is, over all partitions and possible quantization-parameter points will yield to the parameter optimized quantizer, which is by definition the optimal deployment which generate the generalized Voronoi regions as the optimal partition (tessellation[3]). This holds for any density function $\lambda(\omega)$ and target area Ω. To see this[4], let us

---

[3]Since we take here the continuous case, the integral will not distinguish between open or closed sets.

[4]We use the same argumentation as in the prove of [2, Prop.1].

start with any quantizer $(\mathbf{Q}, \mathbf{h}, \mathcal{R})$ for Ω yielding to the average distortion

$$\bar{D}(\mathbf{Q}, \mathbf{h}, \mathcal{R}) = \sum_{n=1}^{N} \int_{\mathcal{R}_n} D(\mathbf{q}_n, h_n, \omega) \lambda(\omega) d\omega \geq \sum_{n=1}^{N} \int_{\mathcal{R}_n} \left(\min_{m \in [N]} D(\mathbf{q}_m, h_n, \omega) \right) \lambda(\omega) d\omega$$

$$= \int_{\Omega} \min_{m \in [N]} D(\mathbf{q}_m, h_n, \omega) \lambda(\omega) d\omega = \sum_{n=1}^{N} \int_{\mathcal{V}_n(\mathbf{Q}, \mathbf{h})} D(\mathbf{q}_n, h_n, \omega) \lambda(\omega) d\omega \qquad (61)$$

where the first inequality is only achieved if for any $\omega \in \mathcal{R}_n$ we have chosen $(\mathbf{q}_n, h_n)$ to be the optimal quantization point with respect to D, or vice versa, if every $(\mathbf{q}, h_n)$ is optimal for every $\omega \in \mathcal{R}_n$, which is the definition of the generalized Voronoi region $\mathcal{V}(\mathbf{Q}, \mathbf{h})$. Therefore, minimizing over all partitions gives equality, i.e.

$$\min_{\mathcal{R}} \bar{D}(\mathbf{Q}, \mathbf{h}, \mathcal{R}) = \bar{D}(\mathbf{Q}, \mathbf{h}, \mathcal{V}(\mathbf{Q}, \mathbf{h})) \qquad (62)$$

for any $(\mathbf{Q}, \mathbf{h}) \in \Omega^N \times \mathbb{R}_+^N$. Hence, we have shown that the parameterized distortion quantizer optimization problem is equivalent to the locational-parameter optimization problem

$$\min_{\mathbf{Q} \in \Omega^N, \mathbf{h} \in \mathbb{R}_+^N} \min_{\mathcal{R} \in \Omega^N} \bar{D}(\mathbf{Q}, \mathbf{h}, \mathcal{R}) = \min_{\mathbf{Q} \in \Omega^N, \mathbf{h} \in \mathbb{R}_+^N} \bar{D}(\mathbf{Q}, \mathbf{h}, \mathcal{V}(\mathbf{Q}, \mathbf{h})) = \bar{D}(\mathbf{Q}^*, \mathbf{h}^*, \mathcal{V}^*). \qquad (63)$$

We need to show that for the optimal $N-$level parameter-quantizer $(\mathbf{Q}^*, \mathbf{h}^*, \mathcal{V}^*)$ with $\mathcal{V}^* = \mathcal{V}(\mathbf{Q}^*, \mathbf{h}^*)$, we have $\mu(\mathcal{V}_n) > 0$ for all $n \in [N]$. Let us first show that each region is indeed a closed interval, i.e., $\mathcal{V}_n^* = [b_{n-1}^*, b_n^*]$ with $0 \leq b_{n-1}^* \leq b_n^* \leq A$.

By the definition of the Möbius regions in Lemma 1, each dominance region is either a single interval (if it is a ball not contained in the target region or a halfspace) or two disjoint intervals (if its a ball contained in the target region), we can not have more than $K_n \leq 2N - 2$ disjoint closed intervals for each Möbius (generalized Voronoi) region. Therefore, the nth optimal Möbius region is given as $\mathcal{V}_n^* = \bigcup_{k=1}^{K_n} v_{n,k}$, where $v_{n,k} = [a_{n,k-1}, a_{n,k}]$ are intervals for some $0 \leq a_{n,k-1} \leq a_{n,k} \leq A$.

Let us assume there are quantization points with disconnected regions, i.e. $K_n > 1$ for $n \in \mathcal{I}_d$ and some $\mathcal{I}_d \subset [N]$. Then, we will re-arrange the partition $\mathcal{V}^*$ by concatenating the K_n disconnected intervals $v_{n,k}$ to $\mathcal{R}_n = [b_{n-1}, b_n]$ for $n \in \mathcal{I}_d$ and move the connected regions appropriatly such that for all $n \in [N]$ it holds $\mu(\mathcal{R}_n) = \mu(\mathcal{V}_n^*) = b_n - b_{n-1}$ and $b_{n-1} \leq b_n$, where we set $b_0 = 0$ and $b_N = A$. For the new concatenated regions, we move each q_n^* to the center of the new arranged regions, i.e., $\tilde{q}_n = \frac{b_n + b_{n-1}}{2}$ for $n \in \mathcal{I}_d$. If for the connected regions $n \in [N] \setminus \mathcal{I}_d$, the quantization point q_n^* is not centroidal, by placing it at the center

of the corresponding closed interval, we will obtain a strictly smaller distortion by Lemma 2.
Hence, for the optimal quantizer, the quantization points must be centroidal and we can assume
$\tilde{q}_n = (b_n + b_{n-1})/2$ for all $n \in [N]$. In this rearrangement, we did not change the parameters h_n^*
at all. The rearranged partition $\mathcal{R} = \{\mathcal{R}_n\}$ and replaced quantization points $\tilde{\mathbf{q}} = (\tilde{q}_1, \ldots, \tilde{q}_N)$
provide the average distortion

$$\bar{D}(\tilde{\mathbf{q}}, \mathbf{h}^*, \mathcal{R}) = \sum_{n=1}^{N} \int_{b_{n-1}}^{b_n} \frac{((\tilde{q}_n - \omega)^2 + h_n^{*2})^\gamma}{h_n^*} d\omega = 2 \sum_{n=1}^{N} \int_0^{\frac{b_n - b_{n-1}}{2}} \frac{(\omega^2 + h_n^{*2})^\gamma}{h_n^*} d\omega \qquad (64)$$

where we substituted ω by $\tilde{q}_n - \omega$. Since the function $(\omega^2 + h_n^{*2})^\gamma$ is strictly monotone increasing
in ω for each $\gamma > 0$, for any $n \in \mathcal{I}_d$, we have

$$\bar{D}_n(\tilde{q}_n, h_n^*, \mathcal{R}_n) = 2 \int_0^{\frac{b_n - b_{n-1}}{2}} \frac{(\omega^2 + h_n^{*2})^\gamma}{h_n^*} d\omega < \sum_{k=1}^{K_n} \int_{a_{n,k} - q_n^*}^{a_{n,k-1} - q_n^*} \frac{(\omega^2 + h_n^{*2})^\gamma}{h_n^*} d\omega \qquad (65)$$

since the non-zero gaps in $\bigcup_k [a_{n,k} - q_n^*, a_{n,k-1} - q_n^*]$ will lead to larger ω in the RHS integral
and therefore to a strictly larger average distortion. Therefore, the points $(\tilde{\mathbf{q}}, \mathbf{h}^*)$ with closed
intervals $\{\mathcal{R}_n\}$ have a strictly smaller average distortion, which contradicts the assumption that
$(\mathbf{q}^*, \mathbf{h}^*)$ is the parameter-optimized quantizer (11). Hence, $K_n = 1$ for each $n \in [N]$ and
every $\gamma \geq 1$. Moreover, the optimal quantization points must be centroids of the intervals, i.e.
$x_n^* = (b_n^* + b_{n-1}^*)/2$.

Now, we have to show that the optimal quantization regions $\mathcal{V}_n^* = \{[b_{n-1}^*, b_n^*]\}_{n=1}^N$ are not
points, i.e., it should hold $b_n^* > b_{n-1}^*$ for each $n \in [N]$. If $b_n^* = b_{n-1}^*$ for some n, then the nth
average distortion $\bar{D}_n$ will be zero for this quantization point, since the integral is vanishing.
But, then we only optimize over $N - 1$ quantization points. So we only need to show that an
additional quantization point strictly decreases the minimum average distortion. Hence, take any
non-zero optimal quantization region $\mathcal{V}_n^* = [b_{n-1}^*, b_n^*]$. We know by Lemma 2 that the optimal
quantizer q_n^* for some closed interval $\mathcal{V}_n^*$ must be centroidal for any parameter h_n. Hence, if
we split $\mathcal{V}_n^*$ with $\mu_n^* = b_n^* - b_{n-1}^*$ by a half and put two quantizers q_{n_1} and q_{n_2} with the same
parameter h_n^* in the center, we will get by using (65)

$$\bar{D}_{n_1} + \bar{D}_{n_2} = \frac{1}{h_n^*} \left(\int_{b_{n-1}^*}^{b_{n-1}^* + \frac{\mu_n^*}{2}} ((q_{n_1} - \omega)^2 + h_n^{*2})^\gamma d\omega + \int_{b_{n-1}^* + \frac{\mu_n^*}{2}}^{b_n^*} ((q_{n_2} - \omega)^2 + h_n^{*2})^\gamma d\omega \right)$$

Substituting $q_{n_i} - \omega$ by ω, we get

$$= \int_{-\frac{\mu_n^*}{4}}^{\frac{\mu_n^*}{4}} \frac{(\omega^2 + h_n^{*2})^\gamma}{h_n^*} d\omega + \int_{-\frac{\mu_n^*}{4}}^{\frac{\mu_n^*}{4}} \frac{(\omega^2 + h_n^{*2})^\gamma}{h_n^*} d\omega \qquad (66)$$

$$= 2\int_0^{\frac{\mu_n^*}{4}} \frac{(\omega^2 + h_n^{*2})^\gamma}{h_n^*} d\omega + w \int_0^{\frac{\mu_n^*}{4}} \frac{(\omega^2 + h_n^{*2})^\gamma}{h_n^*} d\omega \qquad (67)$$

$$< 2\int_0^{\frac{\mu_n^*}{4}} \frac{(\omega^2 + h_n^{*2})^\gamma}{h_n^*} d\omega + 2\int_{\frac{\mu_n^*}{4}}^{\frac{\mu_n^*}{2}} \frac{(\omega^2 + h_n^{*2})^\gamma}{h_n^*} d\omega = 2\int_0^{\frac{\mu_n^*}{2}} \frac{(\omega^2 + h_n^{*2})^\gamma}{h_n^*} d\omega = \bar{D}_n. \quad (68)$$

Hence, the average distortion will strictly decrease if $\mu_n^* > 0$. Therefore, the $N-$level parameter optimized quantizer will have quantization boundaries $b_n > b_{n-1}$ for $n \in [N]$.

APPENDIX C

PROOF OF THEOREM 1

We know by Lemma 3 that the optimal quantization regions are closed non-vanishing intervals $\mathcal{V}_n^* = [b_{n-1}^*, b_n^*]$ for some $b_{n-1}^* < b_n^*$ with quantization points

$$\mathbf{q}_n^* = x_n^* = \frac{b_n^* + b_{n-1}^*}{2} \qquad (69)$$

for $n \in [N]$. Let us set $\mu_n^* = b_n^* - b_{n-1}^*$ for $n \in [N]$. By substituting $\frac{2(x_n^* - \omega)}{\mu_n} = \tilde{\omega}$ and $h_n^* = \frac{u_n^* \mu_n^*}{2}$ in the average distortion, we get

$$\bar{D}(\mathbf{Q}^*, \mathbf{h}^*, \mathcal{V}^*) = \sum_{n=1}^{N} \int_{b_{n-1}^*}^{b_n^*} \frac{((x_n^* - \omega)^2 + h_n^{*2})^\gamma}{h_n^*} \frac{d\omega}{A} = \sum_{n=1}^{N} \int_1^{-1} -\frac{(\mu_n^{*2} \tilde{\omega}^2/4 + u_n^{*2} \mu_n^{*2}/4)^\gamma}{u_n^* \mu_n^*/2} \frac{\mu_n}{2A} d\tilde{\omega}$$

$$= \frac{1}{2^{2\gamma-1}A} \sum_{n=1}^{N} \mu_n^{*2\gamma} \cdot \int_0^1 \frac{(\omega^2 + u_n^{*2})^\gamma}{u_n^*} d\omega \qquad (70)$$

where we used (69) to get for the integral boundaries $2(x_n^* - b_{n-1}^*)/\mu_n^* = 1 = -2(x_n^* - b_n^*)/\mu_n^*$. We do not know the value of u_n^* and μ_n^* but we know that $\mu_n^* > 0$ and $\sum_{n=1}^{N} \mu_n^* = A$ by Lemma 3. Furthermore, (70) is the minimum over all such $\mu_n > 0$ and $u_n > 0$. Hence, it must hold

$$\bar{D}(\mathbf{Q}^*, \mathbf{h}^*, \mathcal{V}^*) = \frac{1}{2^{2\gamma-1}A} \min_{u_n > 0} \min_{\substack{\mu_n > 0 \\ A = \sum_{n=1}^{N} \mu_n}} \sum_{n=1}^{N} \mu_n^{2\gamma} \cdot \left(\int_0^1 \frac{(\omega^2 + u_n^2)^\gamma}{u_n} d\omega \right) = \frac{g(\gamma)}{2^{2\gamma-1}A} \min_{\substack{\mu_n > 0 \\ A = \sum_{n=1}^{N} \mu_n}} \sum_{n=1}^{N} \mu_n^{2\gamma}$$

where in the last equality we used Lemma 2. By the Hölder inequality we get for $p = 2\gamma, q = 2\gamma/(2\gamma - 1)$

$$\sum_{n=1}^{N} \mu_n^{2\gamma} = \sum_{n=1}^{N} \mu_n^p = \sum_{n=1}^{N} \mu_n^p \cdot \Big(\sum_{n=1}^{N} (1/N)^q \Big)^{p/q} \cdot N \geq \Big(\sum_{n=1}^{N} \frac{\mu_n}{N} \Big)^p \cdot N = \Big(\frac{A}{N} \Big)^{2\gamma} N$$

where the equality is achieved if and only if $\mu_n^* = A/N$. Hence, the optimal parameter-quantizer is the uniform scalar quantizer $x_n^* = (2n-1)A/2N$ with identical parameters $h^* = (A/2N)g(\gamma)$ resulting in the minimum average distortion (31).

Let us note here, that for identical parameters, the Möbius regions are closed intervals and reduce to Euclidean Voronoi regions by Lemma 1, for which the optimal tessellation is known to be the uniform scalar quantizer, see for example [26].

References

[1] E. Koyuncu and H. Jafarkhani, "On the minimum distortion of quantizers with heterogeneous reproduction points," *DCC*, Mar. 2016.

[2] ——, "On the minimum average distortion of quantizers with index-dependent distortion measures," *IEEE Transactions on Signal Processing*, vol. 65, no. 17, pp. 4655–4669, Sep. 2017.

[3] E. Koyuncu, R. Khodabakhsh, N. Surya, and H. Seferoglu, "Deployment and trajectory optimization for UAVs: A quantization theory approach," in *2018 IEEE Wireless Communications and Networking Conference (WCNC)*, IEEE, Apr. 2018. eprint: 1708.08832v5.

[4] J.-D. Boissonnat, C. Wormser, and M. Yvinec, "Curved voronoi diagrams," in *Effective Computational Geometry for Curves and Surfaces*. Springer, 2007.

[5] J. Guo and H. Jafarkhani, "Sensor deployment with limited communication range in homogeneous and heterogeneous wireless sensor networks," *IEEE Transactions on Wireless Communications*, vol. 15, no. 10, pp. 6771–6784, Oct. 2016.

[6] J. Guo, E. Koyuncu, and H. Jafarkhani, "A source coding perspective on node deployment in two-tier networks," *IEEE Trans. Commun.*, vol. 66, no. 7, pp. 3035–3049, Jul. 2018.

[7] J. Guo and H. Jafarkhani, "Movement-efficient sensor deployment in wireless sensor networks," *ICC*, May 2018. arXiv: 1710.04746.

[8] M. Moarref and L. Rodrigues, "An optimal control approach to decentralized energy-efficient coverage problems," 3, vol. 47, Elsevier BV, Aug. 2014, pp. 6038–6043.

[9] M. T. Nguyen, L. Rodrigues, C. S. Maniu, and S. Olaru, "Discretized optimal control approach for dynamic multi-agent decentralized coverage," in *ISIC*, Sep. 2016.

[10] B. Galkin, J. Kibilda, and L. A. DaSilva, "Backhaul for low-altitude uavs in urban environments," in *ICC*, May 2018.

[11] M. M. Azari, F. Rosas, and S. Pollin, "Reshaping cellular networks for the sky: Major factors and feasibility," *arxiv*, Oct. 2017.

[12] H. Shakhatreh and A. Khreishah, "Maximizing indoor wireless coverage using uavs equipped with directional antennas," *arxiv*, May 2017.

[13] K. Venugopal, M. C. Valenti, and R. W. Heath, "Device-to-device millimeter wave communications: Interference, coverage, rate, and finite topologies," *IEEE Transactions on Wireless Communications*, vol. 15, no. 9, pp. 6175–6188, Sep. 2016.

[14] H. He, S. Zhang, Y. Zeng, and R. Zhang, "Joint altitude and beamwidth optimization for uav-enabled multiuser communications," *IEEE Commun. Lett.*, vol. 22, no. 2, Feb. 2018.

[15] M. Mozaffari, W. Saad, M. Bennis, and M. Debbah, "Efficient deployment of multiple unmanned aerial vehicles for optimal wireless coverage," *IEEE Commun. Lett.*, vol. 20, no. 8, pp. 1647–1650, Aug. 2016.

[16] A. Goldsmith, *Wireless communications*. Cambridge University Press, 2005.

[17] M. Mozaffari, W. Saad, M. Bennis, and M. Debbah, "Unmanned aerial vehicle with underlaid device-to-device communications: Performance and tradeoffs," *IEEE Transactions on Wireless Communications*, vol. 15, no. 6, pp. 3949–3963, Jun. 2016.

[18] A. Al-Hourani and K. Gomez, "Modeling cellular-to-UAV path-loss for suburban environments," *IEEE Wireless Communications Letters*, vol. 7, no. 1, pp. 82–85, Feb. 2018.

[19] C. A. Balanis, *Antenna theory: Analysis and design*, 3rd ed. Wiley-Interscience, 2005.

[20] A. Okabe, B. Boots, K. Sugihara, and S. N. Chiu, *Spatial tessellations: Concepts and applications of voronoi diagrams*, 2nd ed. John Wiley & Sons, 2000.

[21] J. Cortés, S. Martínez, and F. Bullo, "Spatially-distributed coverage optimization and control with limited-range interactions," *ESAIM*, vol. 11, no. 4, pp. 691–719, Sep. 2005.

[22] J.-D. Boissonnat and M. I. Karavelas, "On the combinatorial complexity of euclidean voronoi cells and convex hulls of d-dimensional spheres," *INRIA*, Jul. 2002.

[23] X. M. Zhang and Y. M. Chu, "Convexity of the integral arithmetic mean of a convex function," *Rocky Mountain Journal of Mathematics*, vol. 40, no. 3, pp. 1061–1068, Jun. 2010.

[24] J. Guo, P. Walk, and H. Jafarkhani, "Quantizers with parameterized distortion measures," *arxiv*, Nov. 2018.

[25] D. Zwillinger, *Standard matehematical tables and formulae*, 31st ed. CRC, 2003.

[26] R. M. Gray and D. L. Neuhoff, "Quantization," *IEEE Transactions on Information Theory*, vol. 44, no. 6, pp. 2325–2383, Oct. 1998.